

Engineer coherent oscillatory modes in Markovian open quantum systems

Chun Hei Leung¹, Pak-Tik Fong², Tianyi Yan¹, and Weibin Li¹

¹*School of Physics and Astronomy and Centre for the Mathematics and Theoretical Physics of Quantum Non-equilibrium Systems, University of Nottingham, Nottingham NG7 2RD, United Kingdom and*

²*Department of Physics, Simon Fraser University, Burnaby, British Columbia V5A 1S6, Canada*

(Dated: March 6, 2026)

We develop a novel framework to engineer persistent oscillatory modes in Markovian open quantum systems governed by a time-independent Lindblad master equation. We show that oscillatory modes can be created when the Hamiltonian and jump operator can be expressed in the same block-diagonal form. A key feature of the framework is that the dissipator of the Lindblad master equation are generally non-zero. We identify the weak and strong conditions, where the onset of the oscillatory modes is dependent and independent of the parameters of the system, respectively. Our method extends beyond the typical decoherence-free subspace approach, in which the dissipator is zero. We demonstrate the applicability of this framework using various models, showing how carefully tailored system-environment interactions can produce sustained coherent oscillations.

I. INTRODUCTION

Understanding the dynamics of open quantum systems is central to modern quantum science, such as solid-state physics [1], quantum thermodynamics [2], quantum biology [3, 4], and quantum chemistry [1, 5, 6]. Insights from the understanding allow to applications in quantum control [7–10], quantum sensing [11–14], and quantum computing [15, 16]. System-environment coupling typically induces dissipation. As a result, the system equilibrates to stationary states, while oscillations are suppressed in the long time limit [17, 18]. Under certain conditions, however, persistent oscillations can survive indefinitely despite continuous environmental coupling [18–27]. Persistent oscillations have been investigated in various models, ranging from collective dissipative spin ensembles [28, 29], synchronization of quantum oscillators [30], dissipative time crystals [31, 32] to quantum scar in thermalized many-body systems [33]. Markovian open quantum systems are typically modeled using the Lindblad master equation [34–36]. Existing theoretical frameworks based on this description have successfully linked the emergence of persistent oscillations to the presence of decoherence-free states [19–24]. In these approaches, the symmetries of the system are identified, which protect the coherent evolution of non-stationary states. One framework requires the existence of decoherence-free subspaces or dark states of the jump operators [22–24, 37], such that the dissipation of states within such a subspace is zero. However, this requires that all states within the subspace be degenerate eigenstates of every jump operator, which is a highly restrictive condition for many practical implementations. Another approach depends on identifying an implicit eigenoperator or symmetry operator of the Liouvillian [19–21]. It predicts a more general condition than the decoherence-free subspace framework because it does not require the persistent oscillation state to be non-dissipative. On the other hand, such operators are not always straightforward to construct, particularly in complex systems. In addition, its connection to decoherence-free subspaces is less transparent. Despite these advances, the search for persistent oscillatory modes in open quantum systems has attracted growing attention.

In this work, we develop a general framework for construct-

ing persistent oscillatory dynamics in Markovian open quantum systems with a time-independent Hamiltonian. The key idea here is that both the jump operator and Hamiltonian can be written in the same block-diagonal form with the same basis. Then, the multiple eigenvalues of the Liouvillian lie on the imaginary axis. Persistent oscillatory modes emerge in the dynamics when initial states overlap with the modes that have non-zero imaginary parts. Our approach not only recovers the connection to the decoherence-free subspace but also shows that persistent oscillations can occur without the existence of decoherence-free states, and can be present when the dissipators do not vanish. Beyond its fundamental significance, the insights gained from this approach open routes to exploit non-stationary quantum technologies, such as autonomous quantum clocks [38–40], by enabling a more flexible and constructive method for generating persistent oscillations and broadening the class of systems capable of supporting such dynamics in the future.

The remainder of this paper is organized as follows. Section II reviews the Lindblad master equation and shows that the dynamical equation supports persistent oscillations. Sec. III A shows the framework connecting persistent oscillations with the decoherence-free subspace. Our generalization to the decoherence-free subspace framework is presented in Sec. III B. In Section IV, we illustrate both frameworks using four examples. The oscillatory behavior observed in the first two examples (Sec. IV A and IV B) is captured by the decoherence-free subspace framework, whereas the oscillations in the latter two examples (Sec. IV C and IV D) can only be explained by our generalized framework but not by the decoherence-free subspace framework. Finally, Section V concludes the paper.

II. LINDBLAD MASTER EQUATION AND LIOUVILLIAN EIGENSPECTRUM

We consider the Markovian Lindblad master equation [34–36], which describes the evolution of a density matrix $\hat{\rho}$,

$$\frac{d}{dt}\hat{\rho} = \mathcal{L}[\hat{\rho}] \equiv -i[\hat{H}, \hat{\rho}] + \sum_i \gamma_i \mathcal{D}_i[\hat{\rho}], \quad (1)$$

where \mathcal{L} is the Liouvillian superoperator, \hat{H} is the system Hamiltonian, and $\mathcal{D}_i[\hat{\rho}] = \hat{L}_i \hat{\rho} \hat{L}_i^\dagger - \frac{1}{2} \hat{L}_i^\dagger \hat{L}_i \hat{\rho} - \frac{1}{2} \hat{\rho} \hat{L}_i^\dagger \hat{L}_i$ is the i -th dissipator with the jump operator \hat{L}_i with damping rate γ_i . When \mathcal{L} is diagonalizable, the solution of Eq. (1) can be expressed [26, 41] as,

$$\hat{\rho}(t) = \sum_k c_k e^{\Lambda_k t} \hat{r}_k, \quad (2)$$

where $c_k \equiv \text{Tr}[\hat{l}_k^\dagger \hat{\rho}(0)]$ is the initial projection amplitude onto the k -th (right) eigenmode. Λ_k , \hat{r}_k , and \hat{l}_k are the Liouvillian eigenvalues, right eigenmodes, and left eigenmodes of the Liouvillian superoperator \mathcal{L} [42–44], respectively. It can be shown that the real part of the Liouvillian eigenvalues is non-positive [45, 46]. Importantly, there always exists an eigenmode r_{SS} with a zero Liouvillian eigenvalue, $\mathcal{L}[r_{\text{SS}}] = 0$, indicating that a steady mode always exists [46–48]. Furthermore, since $\mathcal{L}[\hat{r}_k^\dagger] = (\mathcal{L}[\hat{r}_k])^\dagger$, if \hat{r}_k is an eigenmode with eigenvalue Λ_k , its conjugate $\hat{r}_k^\dagger = \hat{r}_{k'}$ is also an eigenmode, with eigenvalue $\Lambda_{k'} = \Lambda_k^*$.

The Liouvillian eigenspectrum captures the dynamical characteristics of the system. The negative real part of the Liouvillian eigenvalue, $\Gamma_k \equiv -\text{Re}[\Lambda_k]$, determines the decay rate of the k -th eigenmode. Depending on whether the decay rate is zero, the eigenmodes can be categorized into two groups: modes with zero decay rates are undamped, whereas modes with non-zero decay rates are damped. Because of their non-zero decay rates, damped modes gradually decay and eventually vanish, leaving only undamped modes in the long-time dynamics. The imaginary part of the Liouvillian eigenvalue, $\omega_k \equiv \text{Im}[\Lambda_k]$, corresponds to the oscillation frequency. This allows the eigenmodes to be classified into four types: persistent oscillatory, steady, underdamped, and overdamped modes. A comprehensive classification of the eigenmodes is presented in Table I.

TABLE I. The classification of Liouvillian eigenmodes.

	$\Gamma_k \equiv \text{Re}[\Lambda_k] = 0$ ^a	$\Gamma_k \equiv -\text{Re}[\Lambda_k] > 0$ ^b
$\omega_k \equiv \text{Im}[\Lambda_k] \neq 0$	Persistent oscillatory	Underdamped
$\omega_k \equiv \text{Im}[\Lambda_k] = 0$	Steady	Overdamped

^a Undamped modes

^b Damped modes

The persistent oscillatory eigenmodes are of particular interest among the four types of eigenmodes. Instead of reaching a stationary phase in the long-time limit, the observable of the open quantum system exhibits periodic behavior. However, such eigenmodes are typically absent in conventional quantum systems because of inevitable dissipation. In the following, we develop a mathematical framework for engineering open quantum systems that support persistent oscillatory modes.

III. MATHEMATICAL FRAMEWORK

Before presenting our method for constructing persistent oscillatory modes, we first review the decoherence-free frame-

work and the conditions that allow a system to exhibit persistent oscillatory modes in the following section. This is a widely used approach for engineering states in open quantum systems. We then extend these conditions to present our novel generalized result.

A. Decoherence-free Subspaces

We assume that there exists a subspace $\mathcal{W} \subseteq \mathcal{H}$ in Hilbert space \mathcal{H} , which satisfies the following conditions,

1. \mathcal{W} is invariant under \hat{H} , each \hat{L}_i , and each \hat{L}_i^\dagger , i.e.,

$$\hat{H}(\mathcal{W}) \subseteq \mathcal{W}, \quad \hat{L}_i(\mathcal{W}) \subseteq \mathcal{W}, \quad \hat{L}_i^\dagger(\mathcal{W}) \subseteq \mathcal{W}, \quad \forall i,$$

2. The restriction of each jump operator \hat{L}_i to \mathcal{W} is proportional to the identity operator, i.e.

$$\hat{L}_i|_{\mathcal{W}} = \xi_i \mathbb{I}_{\mathcal{W}}, \quad \xi_i \in \mathbb{C}, \quad \forall i.$$

Equivalently, this can be expressed using state $|w\rangle$ that belongs to the subspace \mathcal{W} ,

$$\hat{L}_i|w\rangle = \xi_i|w\rangle, \quad \forall |w\rangle \in \mathcal{W}.$$

Then, \mathcal{W} is a decoherence-free subspace, and the Liouvillian superoperator \mathcal{L} has multiple, undamped modes.

To prove the above statement, it is convenient to work in the eigenbasis \mathcal{E}_H of Hamiltonian \hat{H} . In this basis, each jump operator \hat{L}_i that satisfies the specified conditions can be represented by

$$\hat{L}_i = \left(\xi_i \sum_{\substack{|f\rangle \in \\ \mathcal{E}_H \cap \mathcal{W}}} |f\rangle \langle f| \right) + \sum_{\substack{|p\rangle, |q\rangle \in \\ \mathcal{E}_H \cap \mathcal{W}^\perp}} (\mu_i^{pq} |p\rangle \langle q|), \quad (3)$$

where $\xi_i, \mu_i^{pq} \in \mathbb{C}$ and \mathcal{W}^\perp is the orthogonal complement of \mathcal{W} . In other words, the matrix representation of the jump operators \hat{L}_i in \mathcal{E}_H is,

$$\hat{L}_i = \begin{pmatrix} \xi_i & 0 & 0 & 0 & 0 & 0 \\ 0 & \ddots & 0 & 0 & 0 & 0 \\ 0 & 0 & \xi_i & 0 & 0 & 0 \\ 0 & 0 & 0 & \mu_i^{11} & \mu_i^{12} & \dots \\ 0 & 0 & 0 & \mu_i^{21} & \mu_i^{22} & \dots \\ 0 & 0 & 0 & \vdots & \vdots & \ddots \end{pmatrix}_{\mathcal{E}_H}. \quad (4)$$

Consequently, it can be readily shown that

$$\hat{r}_{u,v} \equiv |u\rangle \langle v|, \quad (5)$$

where $|u\rangle, |v\rangle \in \mathcal{E}_H \cap \mathcal{W}$, renders all dissipators zero,

$$\mathcal{D}_i[\hat{r}_{u,v}] = 0, \quad \forall i. \quad (6)$$

Moreover, $\hat{r}_{u,v}$ are the eigenmodes of the Liouvillian superoperator \mathcal{L} , with eigenvalues $\Lambda_{u,v} = -i(\lambda_u - \lambda_v)$, where λ_u and $\lambda_v \in \mathbb{R}$ are the Hamiltonian eigenvalues corresponding to

the states $|u\rangle$ and $|v\rangle$. In other words, we obtain the following result,

$$\mathcal{L}[\hat{r}_{u,v}] = -i(\lambda_u - \lambda_v) \hat{r}_{u,v}. \quad (7)$$

Because the Liouvillian eigenvalues $\Lambda_{u,v}$ are purely imaginary, the corresponding eigenmodes $\hat{r}_{u,v}$ represent undamped modes. When $\lambda_u \neq \lambda_v$, these modes correspond to persistent oscillatory modes, with frequencies given by the energy gap between the associated Hamiltonian eigenstates. In contrast, when $\lambda_u = \lambda_v$, steady modes are obtained, such as $\hat{r}_{u,u}$ and $\hat{r}_{v,v}$. In both cases, the mode is immune to decay.

B. Generalized framework

In this section, we develop a generalized condition for the existence of persistent oscillatory modes. In contrast to the decoherence-free subspace approach, the dissipator Eq. (6) are generally non-zero in our framework. Under such general conditions, our approach naturally recovers the decoherence-free subspace method, which becomes a special case of the general framework.

Our insight begins by promoting the matrix elements of the jump operators \hat{L}_i in Eq. (4) from scalars to the square matrices. In an appropriate orthonormal basis \mathcal{A} , the jump operators \hat{L}_i and the Hamiltonian \hat{H} can then be expressed in block-diagonal form as,

$$\hat{L}_i = \begin{pmatrix} \Xi_i & \mathbf{0} & \mathbf{0} \\ \mathbf{0} & \Xi_i & \mathbf{0} \\ \mathbf{0} & \mathbf{0} & \mathbf{M}_i \end{pmatrix}_{\mathcal{A}}, \hat{H} = \begin{pmatrix} \mathbf{H}^a & \mathbf{0} & \mathbf{0} \\ \mathbf{0} & \mathbf{H}^b & \mathbf{0} \\ \mathbf{0} & \mathbf{0} & \mathbf{H}^{\text{res}} \end{pmatrix}_{\mathcal{A}}. \quad (8)$$

Here, Ξ_i , \mathbf{H}^a , \mathbf{H}^b are $n \times n$ matrices, while \mathbf{M}_i and \mathbf{H}^{res} are $m \times m$ matrices. Besides, $\mathbf{0}$ denote zero matrices [49].

To streamline the discussion, the \mathbf{M}_i and \mathbf{H}^{res} blocks are omitted in this section without loss of generality. In this simplified setting, the Liouvillian superoperator \mathcal{L} comprises a Hamiltonian \hat{H} and jump operators \hat{L}_i with matrix representations,

$$\hat{H} = \begin{pmatrix} \mathbf{H}^a & \mathbf{0} \\ \mathbf{0} & \mathbf{H}^b \end{pmatrix}_{\mathcal{A}}, \hat{L}_i = \begin{pmatrix} \Xi_i & \mathbf{0} \\ \mathbf{0} & \Xi_i \end{pmatrix}_{\mathcal{A}}. \quad (9)$$

To find the persistent oscillatory mode, we make an ansatz for the eigenmode,

$$\hat{r} = \begin{pmatrix} \mathbf{0} & \mathbf{0} \\ \mathbf{R} & \mathbf{0} \end{pmatrix}_{\mathcal{A}}, \quad (10)$$

where \mathbf{R} is an $n \times n$ matrix. Then, the Liouvillian superoperator acting on the eigenmode \hat{r} yields,

$$\mathcal{L}[\hat{r}] = \begin{pmatrix} \mathbf{0} & \mathbf{0} \\ \mathbf{Q} & \mathbf{0} \end{pmatrix}_{\mathcal{A}}, \quad (11)$$

where the matrix \mathbf{Q} reads,

$$\begin{aligned} \mathbf{Q} &= -i(\mathbf{H}^b \mathbf{R} - \mathbf{R} \mathbf{H}^a) \\ &+ \sum_i \gamma_i (\Xi_i \mathbf{R} \Xi_i^\dagger - \frac{1}{2} \Xi_i^\dagger \Xi_i \mathbf{R} - \frac{1}{2} \mathbf{R} \Xi_i^\dagger \Xi_i) \end{aligned} \quad (12a)$$

$$= i\Delta_{\mathbf{H}} \mathbf{R} + \mathcal{L}^\#[\mathbf{R}]. \quad (12b)$$

Here, $\Delta_{\mathbf{H}} \equiv \mathbf{H}^a - \mathbf{H}^b$, and

$$\mathcal{L}^\#[\mathbf{R}] \equiv -i[\mathbf{H}^a, \mathbf{R}] + \sum_i \gamma_i \mathcal{D}_i^\#[\mathbf{R}], \quad (13a)$$

$$\mathcal{D}_i^\#[\mathbf{R}] \equiv \Xi_i \mathbf{R} \Xi_i^\dagger - \frac{1}{2} \Xi_i^\dagger \Xi_i \mathbf{R} - \frac{1}{2} \mathbf{R} \Xi_i^\dagger \Xi_i. \quad (13b)$$

Since $\mathcal{L}^\#$ is also of Lindbladian form, it is guaranteed to have a steady mode \mathbf{R}_* such that

$$\mathcal{L}^\#[\mathbf{R}_*] = 0. \quad (14)$$

Consequently, if $\mathbf{R} = \mathbf{R}_*$ and \mathbf{R}_* acts as an eigenmode of $\Delta_{\mathbf{H}}$, i.e.,

$$\Delta_{\mathbf{H}} \mathbf{R}_* = \omega \mathbf{R}_* \quad (15)$$

for some non-zero real scalar ω . The corresponding eigenmode \hat{r} is indeed a persistent oscillatory mode with eigenvalue $+i\omega$, i.e.,

$$\mathcal{L}[\hat{r}] = +i\omega \hat{r}. \quad (16)$$

This condition is referred to as the ‘‘weak $\Delta_{\mathbf{H}}$ condition’’. In contrast, we can find an eigenmode $\Delta_{\mathbf{H}}$ that is independent of \mathbf{R}_* ,

$$\Delta_{\mathbf{H}} = \omega \mathbb{I}_n, \quad (17)$$

where \mathbb{I}_n is an n -dimensional identity operator. This gives the so-called ‘‘strong $\Delta_{\mathbf{H}}$ condition’’. Note that ω determines the oscillation frequency of the persistent oscillatory eigenmode \hat{r} . When $\omega = 0$, the oscillatory mode regresses to a steady mode.

As an additional remark, \mathbf{R}_* is generally not unique, and multiple solutions may exist. Nevertheless, at least one of these is Hermitian [46–48]. For this particular Hermitian \mathbf{R}_* , we can find a conjugate persistent oscillatory mode. Its block diagonal form using the same basis reads,

$$\begin{pmatrix} \mathbf{0} & \mathbf{R}_* \\ \mathbf{0} & \mathbf{0} \end{pmatrix}_{\mathcal{A}}. \quad (18)$$

At the same time,

$$\begin{pmatrix} \mathbf{R}_* & \mathbf{0} \\ \mathbf{0} & \mathbf{0} \end{pmatrix}_{\mathcal{A}} \text{ and } \begin{pmatrix} \mathbf{0} & \mathbf{0} \\ \mathbf{0} & \mathbf{R}_* \end{pmatrix}_{\mathcal{A}} \quad (19)$$

represent the steady modes of the Liouvillian \mathcal{L} .

In summary, persistent oscillatory eigenmodes arise when the Hamiltonian \hat{H} and the jump operators \hat{L}_i take the forms specified in Eq. (8), and the relation, $\Delta_{\mathbf{H}} \mathbf{R}_* = \omega \mathbf{R}_*$, is satisfied (in particular, $\Delta_{\mathbf{H}} = \omega \mathbb{I}_n$). Importantly, the construction of the persistent oscillatory mode requires $\mathcal{L}^\#[\mathbf{R}_*] = 0$ but not $\mathcal{D}^\#[\mathbf{R}_*]$, meaning that the dissipator $\mathcal{D}[\hat{r}]$ is non-vanishing in general. The discussion above shows that the decoherence-free subspace method emerges as a special case, i.e. when the dimension n is taken to be 1.

C. Discussion

For the persistent oscillatory modes constructed under the strong $\Delta_{\mathbf{H}}$ condition Eq. (17), the conditions on the Hamiltonian \hat{H} and the jump operators \hat{L}_i can be reformulated as follows. In certain subspace \mathcal{S} , we have

$$\hat{H}|_{\mathcal{S}} = (\mathbb{I}_2 \otimes \mathbf{H}') + \frac{\omega}{2}(\mathbb{Z} \otimes \mathbb{I}_2), \quad (20a)$$

$$\hat{L}_i|_{\mathcal{S}} = \mathbb{I}_2 \otimes \Xi_i, \quad (20b)$$

where \mathbb{Z} is a Pauli Z matrix, and $\mathbf{H}' = \mathbf{H}^a - \frac{\omega}{2}\mathbb{I}_2 = \mathbf{H}^b + \frac{\omega}{2}\mathbb{I}_2$. This formulation can be interpreted as describing a ‘‘two-particle’’ system in which the two particles do not interact and only the second particle experiences dissipation. As a result, the first particle can maintain coherent dynamics, leading to persistent oscillatory behavior in the full system.

This structure is reminiscent of the concept of decoherence-free subsystems. However, our result is not merely a special case of the decoherence-free subsystem framework. Our formulation, particularly the condition on $\Delta_{\mathbf{H}}$ given by Eq. (15) and (17), is complementary to the existing studies. Conventional discussions [50–52] of decoherence-free subsystems typically restrict attention to the structure on jump operators $\hat{L}_i = \mathbb{I}_2 \otimes \Xi_i$ while neglecting the role of Hamiltonian H . It is often focusing on that the subsystem is insensitive to the jump operators \hat{L}_i due to the presence of \mathbb{I}_2 , therefore remains decoherence-free and thus the full system supports coherent dynamics. However, this interpretation does not always provide a complete picture. The Hamiltonian \hat{H} and jump operators \hat{L}_i could play equally essential roles in determining the existence of undamped (persistent oscillatory) dynamics.

In general, a subsystem defined by the jump operator could couple to other parts of the Hilbert space by the Hamiltonian \hat{H} . When the $\Delta_{\mathbf{H}}$ condition is not satisfied by \hat{H} , the existence of persistent oscillatory modes is not guaranteed. One way to resolve this loophole is to require that the Hamiltonian \hat{H} be decoupled. This requirement is precisely what the strong $\Delta_{\mathbf{H}}$ condition Eq. (17) enforces. It is therefore not a mere special case, but a crucial structural requirement ensuring the existence of undamped coherent dynamics.

IV. MODELS EXHIBIT OSCILLATORY MODES

In the following sections, we present four examples of model systems that display persistent oscillatory modes. The first two examples can be understood within the framework of decoherence-free subspaces. The latter two are closely related to our framework. A key difference is that the dissipators associated with these persistent oscillatory modes are non-zero, whereas the decoherence-free subspace framework normally requires their disappearance.

A. Dephasing Quantum Harmonic Oscillator

We begin with a simple example to demonstrate how to construct persistent oscillatory modes using the decoherence-free

subspace method. We consider a harmonic oscillator with the Hamiltonian ($\hbar \equiv 1$) and jump operator given by,

$$\hat{H} = \nu \hat{N} \quad \text{and} \quad \hat{L} = (\hat{N} - 1)^2, \quad (21)$$

where $\hat{N} = \hat{a}^\dagger \hat{a}$ is the number operator with \hat{a}^\dagger (\hat{a}) to be the bosonic creation (annihilation) operator. The oscillator frequency is ν . Since the Fock (number) states $|N\rangle$ are eigenstates of both the Hamiltonian and the jump operator, any subspace formed from these states remains invariant under \hat{H} , \hat{L} , and L^\dagger . Among the Fock states, states $|0\rangle$ and $|2\rangle$ are particularly interesting as,

$$\hat{L}|0\rangle = |0\rangle \quad \text{and} \quad \hat{L}|2\rangle = |2\rangle, \quad (22)$$

This indicates that they form a subspace $\mathcal{W} = \text{span}\{|0\rangle, |2\rangle\}$, which is the decoherence-free subspace of the system. Quantum states described by operators

$$\hat{r}_{0,2} = |0\rangle\langle 2| \quad \text{and} \quad \hat{r}_{2,0} = |2\rangle\langle 0| \quad (23)$$

correspond to the persistent oscillatory modes, with Liouvillian eigenvalues $\Lambda = \mp i2\nu$ and oscillation frequencies $\omega = \mp 2\nu$. One can also find that

$$\hat{r}_{0,0} = |0\rangle\langle 0| \quad \text{and} \quad \hat{r}_{2,2} = |2\rangle\langle 2| \quad (24)$$

are the steady modes. The Liouvillian eigenspectrum shown in Fig. 1 (a) features two purely imaginary Liouvillian eigenvalues that give rise to the two anticipated persistent oscillatory modes.

We now show that the oscillatory modes can be excited in the dissipative dynamics. The system is initialized in a non-trivial superposition of the two states so that its density matrix consists only of oscillatory and steady modes. For example, when the initial state is,

$$|s_{\text{osc}}(0)\rangle = \frac{1}{\sqrt{2}}(|0\rangle + |2\rangle), \quad (25)$$

the initial density matrix reads,

$$\rho_{\text{osc}}(0) = \frac{1}{2}(|0\rangle\langle 2| + |2\rangle\langle 0| + |0\rangle\langle 0| + |2\rangle\langle 2|), \quad (26)$$

which evolves as

$$\rho_{\text{osc}}(t) = \frac{1}{2} \left(e^{i2\nu t} |0\rangle\langle 2| + e^{-i2\nu t} |2\rangle\langle 0| + |0\rangle\langle 0| + |2\rangle\langle 2| \right) \quad (27)$$

The dashed curve in Fig. 1 (b) shows the time evolution of the fidelity $F[\rho_1, \rho_2] \equiv \left(\text{Tr} \sqrt{\sqrt{\rho_1} \rho_2 \sqrt{\rho_1}} \right)^2$ [53] between the density matrix $\rho_{\text{osc}}(t)$ and its initial state $\rho_{\text{osc}}(0)$. The fidelity oscillates at a period $T = \frac{\pi}{\nu}$. The complete revival confirms that the oscillation is persistent.

Alternatively, if the initial state does not lie fully within the decoherence-free subspace, e.g.,

$$|s_{\text{damp}}(0)\rangle = \frac{1}{2}(|0\rangle + |1\rangle + |2\rangle + |3\rangle), \quad (28)$$

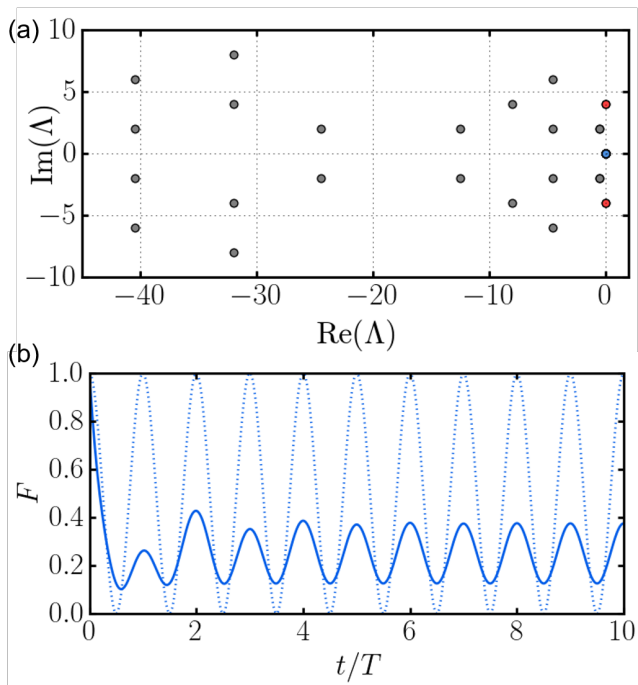


FIG. 1. (a) Liouvillian eigenspectrum. We only show the spectrum near the steady state. The red, blue, and gray points indicate oscillatory, steady, and damped modes, respectively. Notably, the spectrum features an eigenvalue pair at $\pm i4$. (b) Time evolution of fidelities. The dashed curve shows the fidelity between $\rho_{\text{osc}}(t)$ and $\rho_{\text{osc}}(0)$. Solid curve shows the fidelity between $\rho_{\text{damp}}(t)$ and $\rho_{\text{damp}}(0)$. The parameters $\{\nu, \gamma\} = \{2, 1\}$ are used throughout for this Dephasing Quantum Harmonic Oscillator Example, yielding $T = 0.5\pi$.

The system initially exhibited a combination of damped and oscillatory behavior. During the transient period, the damped modes gradually decay. After this period, the dynamics displays the oscillations characteristic of the decoherence-free subspace, as illustrated by the solid curve in Fig. 1 (b).

As an additional remark, although the dephasing jump operator used in this example has been chosen mainly for the sake of simplicity, an experimentally feasible dephasing jump operator version can be realized through nonlinear reservoir engineering [54], yielding the following jump operator,

$$\hat{L} = \sum_{N=0}^{\infty} \mathcal{G}_N(x) |N\rangle \langle N|, \quad (29)$$

which essentially has the same effect. Here, $\mathcal{G}_N(x)$ is the N -th order Laguerre polynomial, and x is a tunable parameter. In particular, there exists an x_* such that $\mathcal{G}_0(x_*) = \mathcal{G}_m(x_*)$ for integer $m > 1$. When $m = 2$, this corresponds to the example discussed in this section.

B. Dephasing spin chain

In this section, we present an example involving multiple jump operators \hat{L}_i and decoherence-free subspaces \mathcal{W}_j . We

consider a three-qubit chain subject to local dephasing on the boundary qubits (the first and third),

$$\hat{L}_1 = \hat{\sigma}_1^z \quad \text{and} \quad \hat{L}_2 = \hat{\sigma}_3^z, \quad (30)$$

Although there is no dephasing in the second qubit, it is coupled to the boundary qubits through an interacting Hamiltonian as follows,

$$\hat{H} = \chi \hat{\sigma}_1^z \hat{\sigma}_2^z \hat{\sigma}_3^z + J_{12} \hat{\sigma}_1^z \hat{\sigma}_2^z + J_{23} \hat{\sigma}_2^z \hat{\sigma}_3^z, \quad (31)$$

where χ is the three-spin interaction strength and J_{ij} is the two-spin interaction strength between the i -th and j -th qubits.

For such system, the Hilbert space \mathcal{H} admits four decoherence-free subspaces \mathcal{W}_j ($j = 1, 2, 3, 4$), as listed in Table II. The restrictions of the two jump operators to each decoherence-free subspace $\hat{L}_i|_{\mathcal{W}_j}$ are equal to either the identity operator or its negative operator. Consequently, each decoherence-free subspace generates two persistent oscillatory modes, yielding a total of eight persistent oscillatory modes, provided that the restriction of the Hamiltonian to each decoherence-free subspace $\hat{H}|_{\mathcal{W}_j}$ is non-degenerate. These modes correspond to $|+j\rangle \langle -j|$ and $|-j\rangle \langle +j|$, where their explicit representations are listed in Table II. Their eigenvalues are $\pm i2(\chi + J_{12} + J_{23})$, $\pm i2(-\chi - J_{12} + J_{23})$, $\pm i2(-\chi + J_{12} - J_{23})$, and $\pm i2(\chi - J_{12} - J_{23})$, respectively. In addition, there is an eight-fold degeneracy at zero Liouvillian eigenvalue, signifying the existence of eight steady modes. These modes form disconnected Hilbert subspace in the dissipative regime [55, 56]. To illustrate the persistent oscillatory modes, we provide an example in Fig. 2. The eight persistent oscillatory modes appear in conjugate pairs.

TABLE II. The fragmentation of the Hilbert space \mathcal{H} .

Subspaces \mathcal{W}_j	$\hat{L}_1 _{\mathcal{W}_j}$	$\hat{L}_2 _{\mathcal{W}_j}$	$\hat{H} _{\mathcal{W}_j}$
$\text{span}[+1\rangle, -1\rangle]$	$+\mathbb{I}$	$+\mathbb{I}$	$(\chi + J_{12} + J_{23}) \sigma_{\mathcal{W}_1}^z$
$\text{span}[+2\rangle, -2\rangle]$	$-\mathbb{I}$	$+\mathbb{I}$	$(-\chi - J_{12} + J_{23}) \sigma_{\mathcal{W}_2}^z$
$\text{span}[+3\rangle, -3\rangle]$	$+\mathbb{I}$	$-\mathbb{I}$	$(-\chi + J_{12} - J_{23}) \sigma_{\mathcal{W}_3}^z$
$\text{span}[+4\rangle, -4\rangle]$	$-\mathbb{I}$	$-\mathbb{I}$	$(\chi - J_{12} - J_{23}) \sigma_{\mathcal{W}_4}^z$

$|+1\rangle = |eee\rangle$, $|-1\rangle = |ege\rangle$, $|+2\rangle = |gee\rangle$, $|-2\rangle = |gge\rangle$,
 $|+3\rangle = |leg\rangle$, $|-3\rangle = |leg\rangle$, $|+4\rangle = |leg\rangle$, $|-4\rangle = |lge\rangle$,
 $\sigma_{\mathcal{W}_j}^z$ is the Pauli-Z operator in the subspace \mathcal{W}_j , $|ijk\rangle$ are the three spins states, with $i, j, k = g, e$, where g and e denote the ground and excited states of the spins, respectively.

C. Spin chain with collective dissipation

In this example, we demonstrate the generalized condition for constructing oscillatory modes. This will be achieved using a three-qubit system. The resulting persistent oscillatory modes cannot be explained within the framework of decoherence-free subspaces because their associated dissipators are non-vanishing. As we will show later, in this example Ξ_i is a 2×2 matrix.

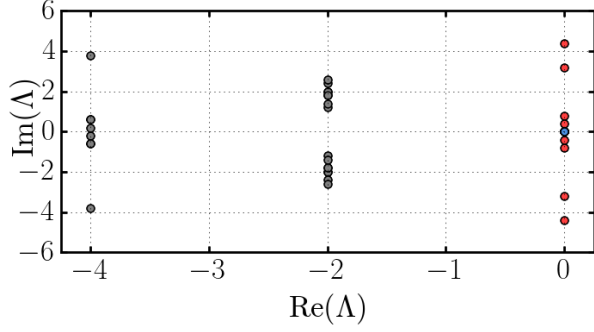


FIG. 2. Liouvillian eigenspectrum. The red, blue, and gray points indicate the oscillatory, steady, and damped modes, respectively. Notably, the spectrum includes eigenvalue pairs located at $\pm i4.4$, $\pm i3.2$, $\pm i0.8$, and $\pm i0.4$. The parameters $\{\chi, J_{12}, J_{23}, \gamma_1, \gamma_2\} = \{0.3, 0.9, 1.0, 1.0, 1.0\}$ are used in the calculation.

Let the jump operator of the system be the collective lowering operator,

$$\hat{L} = \hat{\sigma}_1^- + \hat{\sigma}_2^- + \hat{\sigma}_3^-, \quad (32)$$

where $\hat{\sigma}_i^- = |\downarrow\rangle_i \langle \uparrow|_i$ represents the lowering operator acting on the i -th qubit. In the uncoupled (computational) basis, $\mathcal{B} = \{|\downarrow\downarrow\downarrow\rangle, |\downarrow\downarrow\uparrow\rangle, |\downarrow\uparrow\downarrow\rangle, |\downarrow\uparrow\uparrow\rangle, |\uparrow\downarrow\downarrow\rangle, |\uparrow\downarrow\uparrow\rangle, |\uparrow\uparrow\downarrow\rangle, |\uparrow\uparrow\uparrow\rangle\}$, matrix representation of the jump operator is as follows,

$$\hat{L} = \begin{pmatrix} 0 & 1 & 1 & 0 & 1 & 0 & 0 & 0 \\ 0 & 0 & 0 & 1 & 0 & 1 & 0 & 0 \\ 0 & 0 & 0 & 1 & 0 & 0 & 1 & 0 \\ 0 & 0 & 0 & 0 & 0 & 0 & 0 & 1 \\ 0 & 0 & 0 & 0 & 0 & 1 & 1 & 0 \\ 0 & 0 & 0 & 0 & 0 & 0 & 0 & 1 \\ 0 & 0 & 0 & 0 & 0 & 0 & 0 & 1 \\ 0 & 0 & 0 & 0 & 0 & 0 & 0 & 0 \end{pmatrix}_{\mathcal{B}}. \quad (33)$$

At first glance, it does not exhibit the block-diagonal structure given in Eq. (8). This can be achieved, however, in the coupled basis,

$$C = \left\{ \begin{array}{l} \frac{1}{\sqrt{2}}(|\downarrow\downarrow\uparrow\rangle - |\uparrow\downarrow\downarrow\rangle), \\ \frac{1}{\sqrt{2}}(|\downarrow\uparrow\uparrow\rangle - |\uparrow\uparrow\downarrow\rangle), \\ \hline \frac{-1}{\sqrt{6}}(|\downarrow\downarrow\uparrow\rangle + |\uparrow\downarrow\downarrow\rangle - 2|\downarrow\uparrow\downarrow\rangle), \\ \frac{1}{\sqrt{6}}(|\downarrow\uparrow\uparrow\rangle + |\uparrow\uparrow\downarrow\rangle - 2|\uparrow\downarrow\uparrow\rangle), \\ \hline |\downarrow\downarrow\downarrow\rangle, \\ \frac{1}{\sqrt{3}}(|\downarrow\downarrow\uparrow\rangle + |\downarrow\uparrow\downarrow\rangle + |\uparrow\downarrow\downarrow\rangle), \\ \frac{1}{\sqrt{3}}(|\downarrow\uparrow\uparrow\rangle + |\uparrow\uparrow\downarrow\rangle + |\uparrow\uparrow\downarrow\rangle), \\ \hline |\uparrow\uparrow\uparrow\rangle \end{array} \right\}.$$

The coupled basis is formed by the computational basis and is orthogonal to each other. As the above equation shows, we have either two doublet sectors, and a quartet sector. Using the coupled basis, the matrix representation of the jump operator

reads,

$$\hat{L} = \begin{pmatrix} \boxed{0} & \boxed{1} & 0 & 0 & 0 & 0 & 0 & 0 \\ \boxed{0} & \boxed{0} & 0 & 0 & 0 & 0 & 0 & 0 \\ 0 & 0 & \boxed{0} & \boxed{1} & 0 & 0 & 0 & 0 \\ 0 & 0 & \boxed{0} & \boxed{0} & 0 & 0 & 0 & 0 \\ 0 & 0 & 0 & 0 & 0 & \sqrt{3} & 0 & 0 \\ 0 & 0 & 0 & 0 & 0 & 0 & 2 & 0 \\ 0 & 0 & 0 & 0 & 0 & 0 & 0 & \sqrt{3} \\ 0 & 0 & 0 & 0 & 0 & 0 & 0 & 0 \end{pmatrix}_C. \quad (34)$$

It can be observed that this form has the same structure as that of Eq. (8). Explicitly, it can be seen that the matrix $\Xi = \begin{pmatrix} 0 & 1 \\ 0 & 0 \end{pmatrix}$.

Hamiltonian that can realize the same block-diagonal structure is the three-body Heisenberg XXX model [57–62] with homogeneous external fields, under the open boundary condition [63], which reads,

$$\hat{H} = J \left(\sum_{i=1}^2 \hat{\sigma}_i^x \hat{\sigma}_{i+1}^x + \sum_{i=1}^2 \hat{\sigma}_i^y \hat{\sigma}_{i+1}^y + \sum_{i=1}^2 \hat{\sigma}_i^z \hat{\sigma}_{i+1}^z \right) + h_x \sum_{i=1}^3 \hat{\sigma}_i^x + h_y \sum_{i=1}^3 \hat{\sigma}_i^y + h_z \sum_{i=1}^3 \hat{\sigma}_i^z, \quad (35)$$

$\hat{\sigma}_i^\alpha$ ($\alpha = x, y, z$) are the Pauli operators acting on the i -th qubit, J is the coupling constant, and $h_{x/y/z}$ denote the strength of the external fields along the x , y , and z directions, respectively. To illustrate the block structure, as required by Eq. (8), we give the matrix representation of the Hamiltonian in basis C ,

$$\mathbf{H}^a = \begin{pmatrix} h_z & h_x - i h_y \\ h_x + i h_y & -h_z \end{pmatrix}, \quad (36a)$$

$$\mathbf{H}^b = \begin{pmatrix} -4J + h_z & h_x - i h_y \\ h_x + i h_y & -4J - h_z \end{pmatrix}, \quad (36b)$$

while \mathbf{H}^{res} is a 4×4 matrix, which is not crucial for the persistent oscillatory mode. Therefore its matrix representation is given in Appendix A. One can find straightly that $\Delta_{\mathbf{H}} \equiv \mathbf{H}^a - \mathbf{H}^b = 4J \mathbb{I}_2$, satisfying the strong $\Delta_{\mathbf{H}}$ condition in Eq. (17).

As a result, the Liouvillian \mathcal{L} , which comprises the Hamiltonian in Eq. (35) and the jump operator in Eq. (32), admits a pair of persistent oscillatory eigenmodes. We can explicitly obtain these modes,

$$\hat{r} = \begin{pmatrix} \mathbf{0} & \mathbf{R}_* & \mathbf{0} \\ \mathbf{0} & \mathbf{0} & \mathbf{0} \\ \mathbf{0} & \mathbf{0} & \mathbf{0} \end{pmatrix}_C \quad \text{and} \quad \hat{r}^\dagger = \begin{pmatrix} \mathbf{0} & \mathbf{0} & \mathbf{0} \\ \mathbf{R}_* & \mathbf{0} & \mathbf{0} \\ \mathbf{0} & \mathbf{0} & \mathbf{0} \end{pmatrix}_C, \quad (37)$$

where $\mathbf{R}_* = \frac{8h_x h_z + 2h_y \gamma}{8(h_x^2 + h_y^2 + 2h_z^2) + \gamma^2} \hat{\sigma}^x + \frac{8h_y h_z - 2h_x \gamma}{8(h_x^2 + h_y^2 + 2h_z^2) + \gamma^2} \hat{\sigma}^y + \frac{8h_z^2 + \gamma^2/2}{8(h_x^2 + h_y^2 + 2h_z^2) + \gamma^2} \hat{\sigma}^z + \frac{1}{2} \mathbb{I}_2$. The corresponding eigenvalues are $\Lambda = \mp i4J$. Importantly, their associated dissipators are non-vanishing,

$$\mathcal{D}[\hat{r}] = \begin{pmatrix} \mathbf{0} & \mathbf{D} & \mathbf{0} \\ \mathbf{0} & \mathbf{0} & \mathbf{0} \\ \mathbf{0} & \mathbf{0} & \mathbf{0} \end{pmatrix}_C \neq \mathbf{0}, \quad (38)$$

where $\mathbf{D} = -\frac{4h_x h_z + h_y \gamma}{8(h_x^2 + h_y^2 + 2h_z^2) + \gamma^2} \hat{\sigma}^x - \frac{4h_y h_z - h_x \gamma}{8(h_x^2 + h_y^2 + 2h_z^2) + \gamma^2} \hat{\sigma}^y + \frac{4(h_x^2 + h_y^2)}{8(h_x^2 + h_y^2 + 2h_z^2) + \gamma^2} \hat{\sigma}^z$, and $\mathcal{D}[\hat{\rho}^\dagger] = (\mathcal{D}[\hat{\rho}])^\dagger \neq \mathbf{0}$. It is also worth noting that the existence of these eigenmodes and their oscillation frequencies are independent of the damping rate γ . Fig. 3 (a) shows the Liouvillian eigenspectra. The two purely imaginary Liouvillian eigenvalues at $\Lambda = \pm i4J$ are marked with red dots. The corresponding eigenmodes are the oscillatory states.

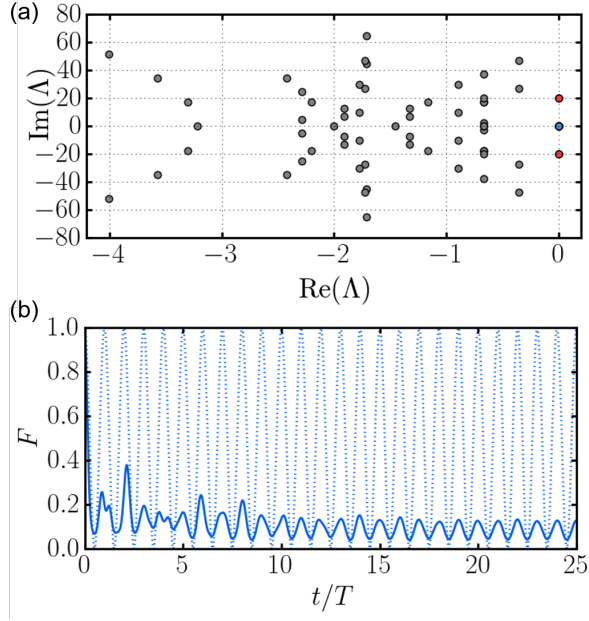


FIG. 3. (a) Liouvillian eigenspectrum. The red, blue, and gray points indicate the persistent oscillatory, steady, and damped modes, respectively. Notably, the spectrum features an eigenvalue pair at $\pm i20$. (b) Time evolution of the fidelities. Dashed curve shows the fidelity between $\rho_{\text{osc}}(t)$ and $\rho_{\text{osc}}(0)$. Solid curve shows the fidelity between $\rho_{\text{damp}}(t)$ and $\rho_{\text{damp}}(0)$. The parameters $\{J, h_x, h_y, h_z, \gamma\} = \{5, 5, 5, 5, 1\}$ are used in the calculation. This yields a period $T = 0.1\pi$ in the oscillation.

Next, we examine the oscillatory dynamics. When the system is initialized in a density matrix composed solely of the persistent oscillatory and steady modes,

$$\rho_{\text{osc}}(0) = \frac{1}{2} \begin{pmatrix} \mathbf{R}_* & \mathbf{R}_* & \mathbf{0} \\ \mathbf{R}_* & \mathbf{R}_* & \mathbf{0} \\ \mathbf{0} & \mathbf{0} & \mathbf{0} \end{pmatrix}_C, \quad (39)$$

the system oscillates back and forth between the initial state $\rho_{\text{osc}}(0)$ and state

$$\rho_{\text{osc}}\left(\frac{T}{2}\right) = \frac{1}{2} \begin{pmatrix} \mathbf{R}_* & -\mathbf{R}_* & \mathbf{0} \\ -\mathbf{R}_* & \mathbf{R}_* & \mathbf{0} \\ \mathbf{0} & \mathbf{0} & \mathbf{0} \end{pmatrix}_C, \quad (40)$$

with period $T = \frac{2\pi}{|\omega|} = \frac{\pi}{2J}$. The dashed curve in Fig. 3(b) shows a numerical simulation of the fidelity between the density matrix $\rho_{\text{osc}}(t)$ and the initial state $\rho_{\text{osc}}(0)$. This result demonstrates that the system returns to the initial state with

perfect fidelity after a period T , indicating that the oscillation is persistent and not influenced by the decoherence.

If the initial density matrix is also constituted of damped modes, for example,

$$\rho_{\text{damp}}(0) = |\downarrow\downarrow\rangle\langle\downarrow\downarrow|, \quad (41)$$

the dynamics does not exhibit complete revival. Once the damped modes have fully decayed, the fidelity oscillates periodically with a lower amplitude. The solid curve in Fig. 3(b) illustrates this case. Initially, the fidelity displays irregular dynamics, but subsequently settles into oscillatory behavior.

Finally, we emphasize that the existence of persistent oscillatory modes is largely independent of the choice of parameters (J, h_x, h_y, h_z , and γ). The only exception is when $J = 0$, in which case the persistent oscillatory modes regress to steady modes.

D. Tuning the Oscillatory Mode

In this example, we demonstrate a case where the strong $\Delta_{\mathbf{H}}$ condition is not satisfied, i.e. $\Delta_{\mathbf{H}} \neq \omega \mathbb{I}_n$. However we can tune the parameter such that the weak $\Delta_{\mathbf{H}}$ condition relation $\Delta_{\mathbf{H}} \mathbf{R}_* = \omega \mathbf{R}_*$ remains satisfied, which generates persistent oscillatory modes. We will discuss the limitations inherent in this construction, which sensitively depend on the parameters.

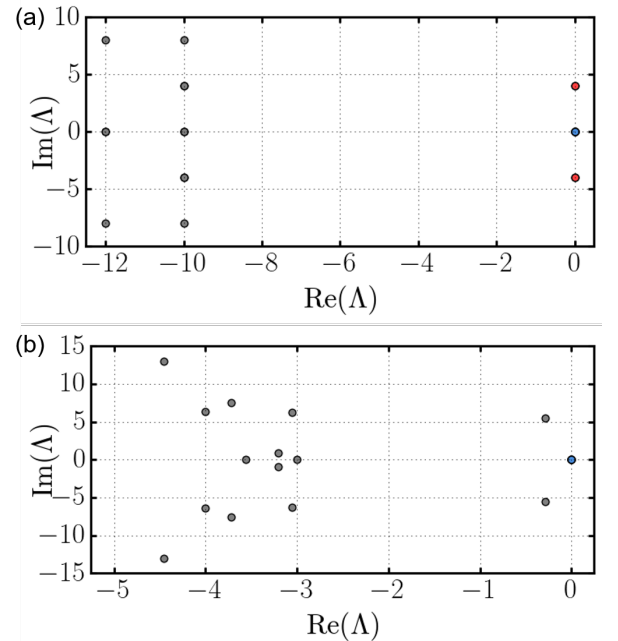


FIG. 4. Liouvillian eigenspectra. The red, blue, and gray points indicate persistent oscillatory, steady, and damped modes, respectively. (a) Parameters $\{E, \gamma_1, \gamma_2\} = \{1, 1, 8\}$. In this case, the spectrum features an eigenvalue pair at $\pm i4$. (b) Parameters $\{E, \gamma_1, \gamma_2\} = \{1, 1, 1\}$. In this case, the spectrum features no purely imaginary eigenvalues.

We consider a two-qubit system with a Liouvillian \mathcal{L} char-

acterized by Hamiltonian

$$\hat{H} = E \left(3\hat{\sigma}_1^z + 6\hat{\sigma}_2^x + \hat{\sigma}_2^y + \hat{\sigma}_1^z \hat{\sigma}_2^y \right), \quad (42)$$

and two jump operators given by,

$$\begin{aligned} \hat{L}_1 &= \left(2 + i\hat{\sigma}_2^x - \hat{\sigma}_2^z \right), \\ \hat{L}_2 &= \frac{1}{2} \left(3 + i\hat{\sigma}_2^x + \hat{\sigma}_2^y - \hat{\sigma}_2^z \right), \end{aligned} \quad (43)$$

where E is the characteristic energy of the system. We will scale the energy with respect to γ_1 . Their matrix representations in the computational basis \mathcal{B} are

$$\hat{H} = E \begin{pmatrix} 3 & 6 - 2i & 0 & 0 \\ 6 + 2i & 3 & 0 & 0 \\ 0 & 0 & -3 & 6 \\ 0 & 0 & 6 & -3 \end{pmatrix}_{\mathcal{B}}, \quad (44)$$

$$\hat{L}_1 = \begin{pmatrix} 1 & i & 0 & 0 \\ i & 3 & 0 & 0 \\ 0 & 0 & 1 & i \\ 0 & 0 & i & 3 \end{pmatrix}_{\mathcal{B}}, \quad \hat{L}_2 = \begin{pmatrix} 1 & 0 & 0 & 0 \\ i & 2 & 0 & 0 \\ 0 & 0 & 1 & 0 \\ 0 & 0 & i & 2 \end{pmatrix}_{\mathcal{B}}. \quad (45)$$

These operators exhibit the block-diagonal structure described in Eq. (8). Using Hamiltonian \hat{H} , one finds that

$$\begin{aligned} \Delta_{\mathbf{H}} &= E \begin{pmatrix} 3 & 6 - 2i \\ 6 + 2i & 3 \end{pmatrix} - E \begin{pmatrix} -3 & 6 \\ 6 & -3 \end{pmatrix} \\ &= E \begin{pmatrix} 6 & -2i \\ 2i & 6 \end{pmatrix}, \end{aligned} \quad (46)$$

which is not proportional to the identity operator. This is in contrast to the previous examples, where the respective $\Delta_{\mathbf{H}}$ is proportional to the identity operator.

Let us now consider a specific choice of parameters, $E = 1$, $\gamma_1 = 1$, and $\gamma_2 = 8$. The steady mode of \mathcal{L}^{\sharp} is $\mathbf{R}_* = \frac{1}{2} \begin{pmatrix} 1 & i \\ -i & 1 \end{pmatrix}$, which satisfies $\Delta_{\mathbf{H}} \mathbf{R}_* = 4\mathbf{R}_*$. Consequently, this configuration supports a pair of persistent oscillatory modes with an oscillation frequency $\omega = \pm 4$. This behavior is confirmed by the Liouvillian eigenspectrum shown in Fig. 4(a), where two purely imaginary eigenvalues, $\Lambda = \pm i4$ are shown. It can also

be verified that the dissipators corresponding to these two persistent oscillatory modes are not zero.

Unlike the previous example (Sec. IV C) the persistent oscillatory modes exist independently of the damping rate γ . The proposed model has fine-tuning sensitivity. Specifically, the presence of oscillatory modes depends critically on the choice of γ_1 and γ_2 . For instance, if we choose $E = 1$, $\gamma_1 = 1$, and $\gamma_2 = 1$, this only gives a steady mode \mathcal{L}^{\sharp} where $\mathbf{R}_* = \frac{1}{251} \begin{pmatrix} 73 & -70 + i52 \\ -70 - i52 & 178 \end{pmatrix}$. As the $\Delta_{\mathbf{H}}$ relation is invalidated, the system does not support persistent oscillatory modes. This can be seen in the corresponding Liouvillian eigenspectrum in Fig. 4(b), where no purely imaginary eigenvalues are found.

V. SUMMARY

We have proposed a theoretical framework for constructing persistent oscillatory modes in Markovian open quantum systems governed by the time-independent Lindblad master equation. Our framework extends beyond the decoherence-free subspace approach. The primary condition for the existence of such modes is that the Hamiltonian \hat{H} and the jump operators \hat{L}_i have a block structure given by Eq. (8). Combined with the weak $\Delta_{\mathbf{H}}$ condition in Eq. (15) facilitates the existence of persistent oscillatory mode. However, these modes are fragile and depend sensitively on the parameters. To overcome this, the strong $\Delta_{\mathbf{H}}$ condition in Eq. (17) can be used, which eliminates dependence on \mathbf{R}_* , thereby avoiding fine-tuning. Under these conditions, the system exhibits oscillatory dynamics even in the presence of dissipation, thus generalizing the concept of decoherence-free subspaces to encompass persistent oscillatory modes. Through the illustrative models, we have demonstrated that appropriately engineered system–environment couplings that satisfy these conditions stabilize long-lived coherent oscillations. This framework provides a systematic route for realizing and controlling long-lived coherent dynamics in open quantum systems. It is interesting to explore how our method can be extended to systems with large number of spins, which may provide insights into the understanding of limit cycle phases in thermodynamic limit [8, 19, 25, 64–71].

Acknowledgments—We thank Yuqiang Liu for helpful discussion. We acknowledge the support from the EPSRC through Grant No. EP/W015641/1 and No. EP/W524402/1. The data that support the findings of this study are openly available [72].

-
- [1] J. Simoni, G. Riva, and Y. Ping, First-principles open quantum dynamics for solids based on density-matrix formalism, *J. Chem. Phys.* **163**, 170901 (2025).
 [2] N. Pathania, D. Tiwari, and S. Banerjee, Quantum thermodynamics of open quantum systems: nature of thermal fluctuations, *Quantum Inf. Process.* **24**, 290 (2025).
 [3] G. Panitchayangkoon, D. Hayes, K. A. Fransted, J. R. Caram, E. Harel, J. Wen, R. E. Blankenship, and G. S. Engel, Long-lived quantum coherence in photosynthetic complexes at phys-

- iological temperature, *Proc. Natl. Acad. Sci. USA* **107**, 12766 (2010).
 [4] M. B. Plenio and S. F. Huelga, Dephasing-assisted transport: quantum networks and biomolecules, *New J. Phys.* **10**, 113019 (2008).
 [5] R. Kapral, Quantum dynamics in open quantum-classical systems, *J. Phys.: Condens. Matter* **27**, 073201 (2015).
 [6] A. Oz, A. Nitzan, O. Hod, and J. E. Peralta, Electron dynamics in open quantum systems: The driven Liouville-von Neumann

- methodology within time-dependent density functional theory, *J. Chem. Theory Comput.* **19**, 7496 (2023).
- [7] C. P. Koch, Controlling open quantum systems: tools, achievements, and limitations, *J. Phys.: Condens. Matter* **28**, 213001 (2016).
- [8] F. Iemini, A. Russomanno, J. Keeling, M. Schirò, M. Dalmonte, and R. Fazio, Boundary time crystals, *Phys. Rev. Lett.* **121**, 035301 (2018).
- [9] M. Koppenhöfer, C. Bruder, and A. Roulet, Quantum synchronization on the IBM Q system, *Phys. Rev. Res.* **2**, 023026 (2020).
- [10] C. A. Weidner, E. A. Reed, J. Monroe, B. Sheller, S. O’Neil, E. Maas, E. A. Jonckheere, F. C. Langbein, and S. Schirmer, Robust quantum control in closed and open systems: Theory and practice, *Automatica* **172**, 111987 (2025).
- [11] V. Montenegro, M. G. Genoni, A. Bayat, and M. G. A. Paris, Quantum metrology with boundary time crystals, *Commun. Phys.* **6**, 304 (2023).
- [12] Y. Jiao, W. Jiang, Y. Zhang, J. Bai, Y. He, H. Shen, J. Zhao, and S. Jia, Observation of multiple time crystals in a driven-dissipative system with Rydberg gas, *Nat. Commun.* **16**, 8767 (2025).
- [13] A. Cabot, F. Carollo, and I. Lesanovsky, Continuous sensing and parameter estimation with the boundary time crystal, *Phys. Rev. Lett.* **132**, 050801 (2024).
- [14] Z. H. Saleem, A. Shaji, and S. K. Gray, Optimal time for sensing in open quantum systems, *Phys. Rev. A* **108**, 022413 (2023).
- [15] P. Zanardi, Dissipation and decoherence in a quantum register, *Phys. Rev. A* **57**, 3276 (1998).
- [16] L. H. C. Vaecairn, J. T. Reilly, J. D. Wilson, S. B. Jäger, and M. Holland, Engineering tunable decoherence-free subspaces with collective atom-cavity interactions, *Phys. Rev. A* **111**, 033718 (2025).
- [17] H. Spohn, An algebraic condition for the approach to equilibrium of an open N-level system, *Lett. Math. Phys.* **2**, 33 (1977).
- [18] P. Menzel and K. Brandner, Limit cycles in periodically driven open quantum systems, *J. Phys. A: Math. Theor.* **52**, 43LT01 (2019).
- [19] B. Buča, J. Tindall, and D. Jaksch, Non-stationary coherent quantum many-body dynamics through dissipation, *Nat. Commun.* **10**, 1730 (2019).
- [20] V. V. Albert and L. Jiang, Symmetries and conserved quantities in Lindblad master equations, *Phys. Rev. A* **89**, 022118 (2014).
- [21] C. Booker, B. Buča, and D. Jaksch, Non-stationarity and dissipative time crystals: spectral properties and finite-size effects, *New J. Phys.* **22**, 085007 (2020).
- [22] H.-R. Wang, D. Yuan, S.-Y. Zhang, Z. Wang, D.-L. Deng, and L.-M. Duan, Embedding quantum many-body scars into decoherence-free subspaces, *Phys. Rev. Lett.* **132**, 150401 (2024).
- [23] B. Buča and T. Prosen, A note on symmetry reductions of the lindblad equation: transport in constrained open spin chains, *New J. Phys.* **14**, 073007 (2012).
- [24] Z. Zhang, J. Tindall, J. Mur-Petit, D. Jaksch, and B. Buča, Stationary state degeneracy of open quantum systems with non-abelian symmetries, *J. Phys. A: Math. Theor.* **53**, 215304 (2020).
- [25] S. Dutta, S. Zhang, and M. Haque, Quantum origin of limit cycles, fixed points, and critical slowing down, *Phys. Rev. Lett.* **134**, 050407 (2025).
- [26] A. Cabot, G. L. Giorgi, and R. Zambrini, Nonequilibrium transition between dissipative time crystals, *PRX Quantum* **5**, 030325 (2024).
- [27] R. I. Karasik, K.-P. Marzlin, B. C. Sanders, and K. B. Whaley, Criteria for dynamically stable decoherence-free subspaces and incoherently generated coherences, *Phys. Rev. A* **77**, 052301 (2008).
- [28] X. Li, Y. Li, and J. Jin, Synchronization of persistent oscillations in spin systems with nonlocal dissipation, *Phys. Rev. A* **107**, 032219 (2023).
- [29] R. Finsterhölzl, M. Katzer, and A. Carmele, Nonequilibrium non-Markovian steady states in open quantum many-body systems: Persistent oscillations in Heisenberg quantum spin chains, *Phys. Rev. B* **102**, 174309 (2020).
- [30] L. Henriot, Environment-induced synchronization of two quantum oscillators, *Phys. Rev. A* **100**, 022119 (2019).
- [31] G. Passarelli, P. Lucignano, R. Fazio, and A. Russomanno, Dissipative time crystals with long-range Lindbladians, *Phys. Rev. B* **106**, 224308 (2022).
- [32] H. Li and W. Yi, Symmetry-induced fragmentation and dissipative time crystal, arXiv preprint, 2501.16592 <https://arxiv.org/abs/2501.16592> (2025).
- [33] M. Serbyn, D. A. Abanin, and Z. Papić, Quantum many-body scars and weak breaking of ergodicity, *Nat. Phys.* **17**, 675 (2021).
- [34] G. Lindblad, On the generators of quantum dynamical semigroups, *Commun. Math. Phys.* **48**, 119 (1976).
- [35] V. Gorini, A. Kossakowski, and E. C. G. Sudarshan, Completely positive dynamical semigroups of N-level systems, *J. Math. Phys.* **17**, 821 (1976).
- [36] F. Nathan and M. S. Rudner, Universal Lindblad equation for open quantum systems, *Phys. Rev. B* **102**, 115109 (2020).
- [37] D. A. Lidar, I. L. Chuang, and K. B. Whaley, Decoherence-free subspaces for quantum computation, *Phys. Rev. Lett.* **81**, 2594 (1998).
- [38] P. Erker, M. T. Mitchison, R. Silva, M. P. Woods, N. Brunner, and M. Huber, Autonomous quantum clocks: Does thermodynamics limit our ability to measure time?, *Phys. Rev. X* **7**, 031022 (2017).
- [39] G. J. Milburn, The thermodynamics of clocks, *Contemp. Phys.* **61**, 69 (2020).
- [40] A. N. Pearson, Y. Guryanova, P. Erker, E. A. Laird, G. A. D. Briggs, M. Huber, and N. Ares, Measuring the thermodynamic cost of timekeeping, *Phys. Rev. X* **11**, 021029 (2021).
- [41] F. Minganti, A. Biella, N. Bartolo, and C. Ciuti, Spectral theory of Liouvillians for dissipative phase transitions, *Phys. Rev. A* **98**, 042118 (2018).
- [42] Y.-L. Zhou, X.-D. Yu, C.-W. Wu, X.-Q. Li, J. Zhang, W. Li, and P.-X. Chen, Accelerating relaxation through liouvillian exceptional point, *Phys. Rev. Res.* **5**, 043036 (2023).
- [43] S. Longhi, Quantum Mpemba Effect from Non-Normal Dynamics, *Entropy* **27**, 581 (2025).
- [44] J. Zhang, G. Xia, C.-W. Wu, T. Chen, Q. Zhang, Y. Xie, W.-B. Su, W. Wu, C.-W. Qiu, P.-X. Chen, W. Li, H. Jing, and Y.-L. Zhou, Observation of quantum strong Mpemba effect, *Nat Commun* **16**, 301 (2025).
- [45] Y. Zhang and T. Barthel, A direct algebraic proof for the non-positivity of Liouvillian eigenvalues in Markovian quantum dynamics, arXiv preprint, arXiv:2504.02256 (2025).
- [46] B. Baumgartner and H. Narnhofer, Analysis of quantum semigroups with GKS-Lindblad generators: II. General, *J. Phys. A: Math. Theor.* **41**, 395303 (2008).
- [47] A. Rivas and S. F. Huelga, Quantum Markov process: Mathematical structure, in *Open Quantum Systems: An Introduction* (Springer Berlin Heidelberg, Berlin, Heidelberg, 2012) pp. 33–48.
- [48] D. E. Evans, Irreducible quantum dynamical semigroups, *Commun. Math. Phys.* **54**, 293 (1977).

- [49] For simplicity, the dimensions of the zero matrices are not explicitly indicated, as they vary throughout the paper. However, their sizes can be inferred from the surrounding context.
- [50] J. Kempe, D. Bacon, D. A. Lidar, and K. B. Whaley, Theory of decoherence-free fault-tolerant universal quantum computation, *Phys. Rev. A* **63**, 042307 (2001).
- [51] D. A. Lidar and K. Birgitta Whaley, Decoherence-free subspaces and subsystems, in *Irreversible Quantum Dynamics*, edited by F. Benatti and R. Floreanini (Springer Berlin Heidelberg, Berlin, Heidelberg, 2003) pp. 83–120.
- [52] S. Dutta, An introduction to markovian open quantum systems, [arXiv preprint,2510.26530](#) (2025).
- [53] R. Jozsa, Fidelity for mixed quantum states, *J. Mod. Opt.* **41**, 2315 (1994).
- [54] I. Rojtkov, M. Simoni, E. Zapusek, F. Reiter, and J. Home, Stabilization of cat-state manifolds using nonlinear reservoir engineering, [arXiv preprint, arXiv:2407.18087](#) (2025).
- [55] T. Yan, C. H. Leung, and W. Li, Hilbert space fragmentation in driven-dephasing Rydberg atom array, [arXiv preprint, arXiv:2511.23395](#) (2025).
- [56] Y. Li, P. Sala, and F. Pollmann, Hilbert space fragmentation in open quantum systems, *Phys. Rev. Res.* **5**, 043239 (2023).
- [57] W. Heisenberg, Zur theorie des ferromagnetismus, *Z. Phys.* **49**, 619 (1928).
- [58] L. A. Takhtajan, The quantum inverse problem method and the XYZ Heisenberg model, *Physica D* **3**, 231 (1981).
- [59] R. J. Baxter, Partition function of the eight-vertex lattice model, *Ann. Phys.* **70**, 193 (1972).
- [60] Y. Guo-Hui, G. Wen-Bin, Z. Ling, and S. He-Shan, Entanglement in anisotropic Heisenberg XYZ chain with inhomogeneous magnetic field, *Commun. Theor. Phys.* **48**, 453 (2007).
- [61] A. Abliz, H. J. Gao, X. C. Xie, Y. S. Wu, and W. M. Liu, Entanglement control in an anisotropic two-qubit Heisenberg XYZ model with external magnetic fields, *Phys. Rev. A* **74**, 052105 (2006).
- [62] P. Thakur and P. Durganandini, Heisenberg spin-1/2 XXZ chain in the presence of electric and magnetic fields, *Phys. Rev. B* **97**, 064413 (2018).
- [63] If periodic boundary condition is applied instead, the pair of persistent oscillatory modes regresses to two steady modes, due to the fact that the Hamiltonian becomes degenerated. Nevertheless, the pair of persistent oscillatory modes can be recovered if an additional boundary term is included. A detailed discussion of this scenario is provided in Appendix B.
- [64] C.-K. Chan, T. E. Lee, and S. Gopalakrishnan, Limit-cycle phase in driven-dissipative spin systems, *Phys. Rev. A* **91**, 051601 (2015).
- [65] K. Seibold, R. Rota, and V. Savona, Dissipative time crystal in an asymmetric nonlinear photonic dimer, *Phys. Rev. A* **101**, 033839 (2020).
- [66] L. R. Bakker, M. S. Bahovadinov, D. V. Kurlov, V. Gritsev, A. K. Fedorov, and D. O. Krimer, Driven-dissipative time crystalline phases in a two-mode bosonic system with kerr nonlinearity, *Phys. Rev. Lett.* **129**, 250401 (2022).
- [67] P. Kongkhambut, J. Skulte, L. Mathey, J. G. Cosme, A. Hemmerich, and H. Keßler, Observation of a continuous time crystal, *Science* **377**, 670 (2022).
- [68] K. Wadenpfuhl and C. S. Adams, Emergence of synchronization in a driven-dissipative hot Rydberg vapor, *Phys. Rev. Lett.* **131**, 143002 (2023).
- [69] D. Ding, Z. Bai, Z. Liu, B. Shi, G. Guo, W. Li, and C. S. Adams, Ergodicity breaking from Rydberg clusters in a driven-dissipative many-body system, *Sci. Adv.* **10**, ead15893 (2024).
- [70] X. Wu, Z. Wang, F. Yang, R. Gao, C. Liang, M. K. Tey, X. Li, T. Pohl, and L. You, Dissipative time crystal in a strongly interacting Rydberg gas, *Nat. Phys.* **20**, 1389 (2024).
- [71] Y.-X. Xiang, Q.-L. Lei, Z. Bai, and Y.-Q. Ma, Self-organized time crystal in driven-dissipative quantum system, *Phys. Rev. Res.* **6**, 033185 (2024).
- [72] C. H. Leung, T. Yan, and W. Li, Engineer coherent oscillatory modes in markovian open quantum systems, [10.5281/zenodo.17866420](#) (2025).

Appendix A: Matrix form of the Hamiltonian for the spin chain with collective dissipation

The matrix form of Hamiltonian Eq. (35) can be written in the coupled basis C ,

$$\hat{H} = \begin{pmatrix} \mathbf{H}^a & \mathbf{0} & \mathbf{0} \\ \mathbf{0} & \mathbf{H}^b & \mathbf{0} \\ \mathbf{0} & \mathbf{0} & \mathbf{H}^{\text{res}} \end{pmatrix}_C, \quad (\text{A1})$$

where the three blocks in the Hamiltonian read,

$$\mathbf{H}^a = \begin{pmatrix} h_z & h_x - \text{i}h_y \\ h_x + \text{i}h_y & -h_z \end{pmatrix}, \quad (\text{A2a})$$

$$\mathbf{H}^b = \begin{pmatrix} -4J + h_z & h_x - \text{i}h_y \\ h_x + \text{i}h_y & -4J - h_z \end{pmatrix}, \quad (\text{A2b})$$

$$\mathbf{H}^{\text{res}} = \begin{pmatrix} 4J + 3h_z & \sqrt{3}(h_x - \text{i}h_y) & 0 & 0 \\ \sqrt{3}(h_x + \text{i}h_y) & 4J + h_z & 2(h_x - \text{i}h_y) & 0 \\ 0 & 2(h_x + \text{i}h_y) & 4J - h_z & \sqrt{3}(h_x - \text{i}h_y) \\ 0 & 0 & \sqrt{3}(h_x + \text{i}h_y) & 4J - 3h_z \end{pmatrix}. \quad (\text{A2c})$$

Appendix B: Heisenberg XYZ chain with periodic condition

The Hamiltonian of a Heisenberg XYZ model with the periodic boundary condition can cooperate with the collective lowering jump operator \hat{L} as follows: (32) such that oscillatory modes are enabled. The explicit form of the Hamiltonian for three qubits under the periodic boundary condition reads,

$$\hat{H}_{\text{peri-XYZ}} = \hat{H}_{\text{coup}} + \hat{H}_{\text{ext}} \quad (\text{B1})$$

where

$$\hat{H}_{\text{coup}} = J_x \sum_{i=1}^3 \hat{\sigma}_i^x \hat{\sigma}_{i+1}^x + J_y \sum_{i=1}^3 \hat{\sigma}_i^y \hat{\sigma}_{i+1}^y + J_z \sum_{i=1}^3 \hat{\sigma}_i^z \hat{\sigma}_{i+1}^z, \quad (\text{B2a})$$

$$\hat{H}_{\text{ext}} = h_x \sum_{i=1}^3 \hat{\sigma}_i^x + h_y \sum_{i=1}^3 \hat{\sigma}_i^y + h_z \sum_{i=1}^3 \hat{\sigma}_i^z, \quad (\text{B2b})$$

and $\hat{\sigma}_{i=4}^{x/y/z} \equiv \hat{\sigma}_{i=1}^{x/y/z}$. Its matrix representation in basis C is given by

$$\hat{H}_{\text{peri-XYZ}} = \begin{pmatrix} \hat{\mathbf{H}}_{\text{peri-XYZ}}^a & \mathbf{0} & \mathbf{0} \\ \mathbf{0} & \mathbf{H}_{\text{peri-XYZ}}^b & \mathbf{0} \\ \mathbf{0} & \mathbf{0} & \mathbf{H}_{\text{peri-XYZ}}^{\text{res}} \end{pmatrix}_C, \quad (\text{B3})$$

where

$$\mathbf{H}_{\text{peri-XYZ}}^a = \begin{pmatrix} -J_x - J_y - J_z + h_z & h_x - \text{i}h_y \\ h_x + \text{i}h_y & -J_x - J_y - J_z - h_z \end{pmatrix}, \quad (\text{B4a})$$

$$\mathbf{H}_{\text{peri-XYZ}}^b = \begin{pmatrix} -J_x - J_y - J_z + h_z & h_x - \text{i}h_y \\ h_x + \text{i}h_y & -J_x - J_y - J_z - h_z \end{pmatrix}, \quad (\text{B4b})$$

$$\mathbf{H}_{\text{peri-XYZ}}^{\text{res}} = \begin{pmatrix} 3J_z + 3h_z & \sqrt{3}(h_x - \text{i}h_y) & \sqrt{3}(J_x - J_y) & 0 \\ \sqrt{3}(h_x + \text{i}h_y) & 2J_x + 2J_y - J_z + h_z & 2(h_x - \text{i}h_y) & \sqrt{3}(J_x - J_y) \\ \sqrt{3}(J_x - J_y) & 2(h_x + \text{i}h_y) & 2J_x + 2J_y - J_z - h_z & \sqrt{3}(h_x - \text{i}h_y) \\ 0 & \sqrt{3}(J_x - J_y) & \sqrt{3}(h_x + \text{i}h_y) & 3J_z - 3h_z \end{pmatrix}. \quad (\text{B4c})$$

Hence, $\Delta_{\mathbf{H}} \equiv \mathbf{H}_{\text{peri-XYZ}}^a - \mathbf{H}_{\text{peri-XYZ}}^b = \mathbf{0}$, and the pair of persistent oscillatory modes is regressed to two steady modes.

To recover the oscillatory modes, the Hamiltonian must be non-degenerate. This can be achieved by adding a boundary term H_{boun} ,

$$\hat{H}_{\text{asym.peri.XYZ}} = \hat{H}_{\text{peri.XYZ}} + \hat{H}_{\text{boun}}, \quad (\text{B5})$$

where

$$\hat{H}_{\text{boun}} = -\frac{\Omega}{4}(\hat{\sigma}_1^x \hat{\sigma}_3^x + \hat{\sigma}_1^y \hat{\sigma}_3^y + \hat{\sigma}_1^z \hat{\sigma}_3^z). \quad (\text{B6})$$

Its matrix representation in basis \mathcal{C} is given by

$$\hat{H}_{\text{asym.peri.XYZ}} = \begin{pmatrix} \mathbf{H}_{\text{asym.peri.XYZ}}^{\mathbf{a}} & \mathbf{0} & \mathbf{0} \\ \mathbf{0} & \mathbf{H}_{\text{asym.peri.XYZ}}^{\mathbf{b}} & \mathbf{0} \\ \mathbf{0} & \mathbf{0} & \mathbf{H}_{\text{asym.peri.XYZ}}^{\text{res}} \end{pmatrix}_{\mathcal{C}}, \quad (\text{B7})$$

where

$$\mathbf{H}_{\text{asym.peri.XYZ}}^{\mathbf{a}} = \begin{pmatrix} -J_x - J_y - J_z + h_z + \frac{3}{4}\Omega & h_x - \text{i}h_y \\ h_x + \text{i}h_y & -J_x - J_y - J_z - h_z + \frac{3}{4}\Omega \end{pmatrix}, \quad (\text{B8a})$$

$$\mathbf{H}_{\text{asym.peri.XYZ}}^{\mathbf{b}} = \begin{pmatrix} -J_x - J_y - J_z + h_z - \frac{1}{4}\Omega & h_x - \text{i}h_y \\ h_x + \text{i}h_y & -J_x - J_y - J_z - h_z - \frac{1}{4}\Omega \end{pmatrix}, \quad (\text{B8b})$$

$$\mathbf{H}_{\text{asym.peri.XYZ}}^{\text{res}} = \begin{pmatrix} 3J_z + 3h_z + \frac{1}{4}\Omega & \sqrt{3}(h_x - \text{i}h_y) & \sqrt{3}(J_x - J_y) & 0 \\ \sqrt{3}(h_x + \text{i}h_y) & 2J_x + 2J_y - J_z + h_z + \frac{1}{4}\Omega & 2(h_x - \text{i}h_y) & \sqrt{3}(J_x - J_y) \\ \sqrt{3}(J_x - J_y) & 2(h_x + \text{i}h_y) & 2J_x + 2J_y - J_z - h_z + \frac{1}{4}\Omega & \sqrt{3}(h_x - \text{i}h_y) \\ 0 & \sqrt{3}(J_x - J_y) & \sqrt{3}(h_x + \text{i}h_y) & 3J_z - 3h_z + \frac{1}{4}\Omega \end{pmatrix}. \quad (\text{B8c})$$

Hence, $\Delta_{\mathbf{H}} \equiv \mathbf{H}_{\text{asym.peri.XYZ}}^{\mathbf{a}} - \mathbf{H}_{\text{asym.peri.XYZ}}^{\mathbf{b}} = \Omega \mathbb{I}_2$. Consequently, we obtain a pair of oscillatory modes with eigenvalues $\Lambda = \mp \text{i}\Omega$. The amplitude of the boundary term \hat{H}_{boun} determines the (angular) oscillation frequency $\omega = \mp \Omega$. It reduces to the open boundary Heisenberg XXX model with a homogeneous external field Eq. (35) when $J_x = J_y = J_z = J$ and $\Omega = 4J$.